Geoderma 385 (2021) 114834

Contents lists available at ScienceDirect

Geoderma

journal homepage: www.elsevier.com/locate/geoderma

Comparison of different methods for assessing effects of soil interparticle forces on aggregate stability

Jingfang Liu[a], Feinan Hu[a,b,*], Chenyang Xu[a], Zilong Wang[a], Rentian Ma[a], Shiwei Zhao[a,b], Gang Liu[a,b]

[a] State Key Laboratory of Soil Erosion and Dryland Farming on the Loess Plateau, College of Natural Resources and Environment, Northwest A&F University, Yangling 712100, China

[b] Institute of Soil and Water Conservation, Chinese Academy of Sciences and Ministry of Water Resources, Yangling 712100, China

ARTICLE INFO

Handling Editor: Morgan Cristine L.S.

Keywords:
Aggregate stability
Electrostatic repulsive force
Van der Waals force
Raindrop impact
Rainfall simulation

ABSTRACT

Soil interparticle forces, involving in van der Waals attractive force, and surface hydration and electrostatic repulsive forces, greatly influence the soil aggregate stability. However, current studies on methods for evaluating the impact of soil interparticle forces in aggregate stability are scarce. This research was aimed to examine the impact of soil interparticle forces on aggregate stability using diverse methods for different soil types. Soil aggregate stability was tested through the pipette method, wet sieving, and rainfall simulation, respectively characterized by aggregate stability index (ASI), mean weight diameter (MWD), and splash erosion mass (SE). Soil interparticle forces were adjusted by the changing concentrations of NaCl solution. The results showed that all three approaches can be applied to study the impact of soil interparticle forces on aggregate stability. The ASI, MWD, and SE showed little change below 10^{-2} mol L^{-1} NaCl concentration and then ASI and MWD increased at a high rate above 10^{-2} mol L^{-1} concentration of NaCl, while the SE showed the opposite trend. These results were as expected for soil interparticle forces. Moreover, for a single soil, a substantial correlation existed between the aggregate stability indicators obtained from three methods. However, the order of soil aggregate stability, measured by three methods were varied among soil types. Our results suggest that a single method cannot be applied to determine the aggregate stability of all soil types even if the breakdown mechanism was identical, because organic matter content and particle size distribution of soil are important factors influencing aggregate stability. Hence, in order to compare the difference in aggregate stability between various soils, multiple methods should be considered to investigate the impact of interparticle forces of soil on its aggregate stability. If a single method was to be chosen, wet sieving may be a good choice as it was not only relatively simple and time-saving but also reflected more comprehensive information about sizes and amount of fragments released from soil aggregates.

1. Introduction

The potential of the aggregates to resist disaggregation when subjected to destructive pressures is termed as soil aggregate stability and it is extensively utilized as an indicator of erodibility and health of the soil. Aggregate breaking is considered as a key step in soil erosion (Legout et al., 2005; Vaezi et al., 2017; Fernández-Raga, et al., 2018). When rainfall enters the soil, aggregates break up into fine particles, which results in the clogging of soil pores, surface crusting, reducing water infiltration, and thus leading to the increasing surface runoff and soil erosion (Barthès and Roose, 2002; Horn and Smucker, 2005; Cantón et al., 2009; Falsone et al., 2012; Vaezi et al., 2017). Therefore, the evaluation of soil aggregate stability is vital to understand the process related to soil and water at the macro scale.

Currently, four main mechanisms are widely recognised as the reasons for the soil aggregate breakdown (Le Bissonnais, 1996). These include differential swelling, slaking effect, raindrop impact, and osmotic stress. According to previous studies, the pressure strength produced by above mechanisms was lower than 3 atm (Nearing et al., 1987; Levy et al., 2003; Xu et al., 2015), which seem too weak to break the soil

* Corresponding author at: State Key Laboratory of Soil Erosion and Dryland Farming on the Loess Plateau, College of Natural Resources and Environment, Northwest A&F University, Yangling 712100, China.

E-mail address: hufn@nwafu.edu.cn (F. Hu).

https://doi.org/10.1016/j.geoderma.2020.114834
Received 25 July 2020; Received in revised form 16 October 2020; Accepted 8 November 2020
Available online 1 December 2020

aggregates. However, latest published literatures have revealed that the pressure produced by soil interparticle forces could reach as high 100–1000 atm (Li et al., 2013; Yu et al., 2017, 2020a; Hu et al., 2018a, 2018b), which was strong enough to destroy the aggregates. Soil interparticle forces comprise of van der Waals attractive and hydration, electrostatic repulsive forces. Among these soil interparticle forces, the attractive force is responsible to resist the aggregate dispersion (Liang et al., 2007; Xu et al., 2015; Huang et al., 2016). In contrast, the breakdown of soil aggregates is associated with repulsive forces (McBride and Baveye, 2002; Leng, 2012; Li et al., 2013). The sum of the repulsive and attractive forces determine the aggregate stability during wetting (Hu et al., 2015; Yu et al., 2020b). At present, considerable studies have stressed the important influence of soil interparticle forces on the stability of its aggregate, however, methods for evaluating their effects on soil aggregate stability applied by these studies are limited.

There are many methods for measuring water stability of soil aggregates, such as wet sieving, ultrasonic vibration, turbidimetric techniques, and rainfall simulation (Yoder, 1936; Quirk, 1950; Bruce-Okine and Lal, 1975; Le Bissonnais, 1996; Zhu et al., 2009; Pulido Moncada et al., 2015; Almajmaie et al., 2017). Numerous researches have reported that the results of aggregate stability showed significant differences among the various methods as the different methods simulated the different mechanism and the energy applied by methods were arbitrary or even do not existed in the field. (Amézketa, 1999; Herrick et al., 2001; Pulido Moncada et al., 2015; Saygin et al., 2015). For example, ultrasonic vibration cannot be related to the behavior of field soils (Almajmaie et al., 2017). Wet sieving tends to amplify the slaking effects (Kemper and Rosenau, 1986), whereas rainfall simulation stresses the mechanical raindrop impact force. In order to distinguish different mechanisms of aggregate breakdown, Le Bissonnais (1996) proposed a unified method with three pre-treatments, including mechanical breakdown, fast wetting, and slow wetting. However, this method was not be extensively applied due to its complicated procedures and the absence of raindrop impact mechanism. Considering that the method selected should be simple, easily replicated and well reflects the natural condition, wet sieving and rainfall simulation were the most common methods adopted by researches to assess aggregate stability (Amézketa, 1999; Rohoskova, 2004; Pulido Moncada et al., 2015; Saygin et al., 2015; Almajmaie et al., 2017). In contrast, the influence of soil interparticle forces on aggregate stability were always studied using the pipette method, which through measuring fine soil particles of the suspension after the fast wetting process (Le Bissonnais, 1996; Li et al., 2013; Hu et al., 2015; Huang et al., 2016; Yu et al., 2020a). Whether these common methods measuring the aggregate water stability can be applied to test the effect of soil interparticle forces on aggregate stability are still not clear. Therefore, it is necessary to apply various methods to study the aggregate stability subjected to soil interparticle forces.

The Loess Plateau is one of the most serious regions of soil erosion in China. In this study, four typical soils in this region were selected to (1) study the impact of soil interparticle forces on aggregate stability using multiple methods, (2) compare the effect of these methods on aggregate stability of different soil types, (3) provide a reference to select the methods to measure the aggregate stability.

2. Materials and methods

2.1. Soil sampling

We collected the soil samples from Ansai (109°19′21″E, 36°51′50″N), Chunhua (108°30′07″E, 34°56′29″N), Yangling (108°02′30″E, 34°18′14″N), and Zhouzhi (108°03′10″E, 34°08′08″N), in the Shaanxi Province, China. In this region, the major crops planted are winter wheat (*Triticum aestivum Linn*), broom corn millet (*Panicum miliaceum L*), and maize (*Zea mays* L). Loessal soil, Heilu soil, Lou soil, and Cinnamon soil are included in this study. The selected soils are widely distributed in the Loess Plateau and are all developed from loess parent materials. For each soil type, samples were collected from the top 0–20 cm layer of three representative cultivated lands. According to the FAO soil classification, Loessal soil and Lou soil are classified as Calcic Cambisols, whereas Cinnamon soil and Heilu soil are classified as Lixisols and Chernozems, respectively. Soil texture for Lou soil and Cinnamon soil is loamy clay, while it is sandy loam for Loessal soil and clay loam for Heilu soil based on the International System of Soil Texture Classification.

Soil basic physio-chemical features are listed in Table 1. Soil organic matter (SOM) was tested using the $K_2Cr_2O_7$ oxidation method. Soil pH (solution/soil ratio: 5:1) was measured using a pH electrode. Cation exchange capacity (CEC) and specific surface area (SSA) were analyzed as described by Li et al. (2011). The laser diffractometer of Malvern Mastersizer 2000 (Malvern Instruments Ltd., UK) was utilized to measure particle size distributions, and soil pre-treatment was conducted according to the study of Yang et al. (2015). The main clay minerals in the soils were hydromica, kaolinite, chlorite, which were determined by X-ray diffraction.

2.2. Sample preparation

For the quantitative assessment about impacts of soil interparticle forces on aggregate stability, soils were first exchanged with a single cation species. As described in earlier published studies (Huang et al., 2016; Ding et al., 2019), weak polarization of Na^+ at the colloidal interface of soil was considered as a most suitable strategy to investigate the impact of interparticle forces of soil on its aggregate stability. Hence, the soil specimens were made Na^+-saturated for the utilization in the present work. The procedures for preparing Na^+-saturated soil samples is based on the study of Xu et al. (2015). Briefly, air-dried soil samples were subjected for washing by dispersion, agitation, centrifugation, and decantation with NaCl solution, and followed by washing with deionized water for the removal of free Na^+ from the suspension. Finally, samples were subjected to oven drying at 60 °C, crushed and sieved to obtain model aggregates of diameter 1–5 mm for the assessment of aggregate stability.

2.3. Determination of aggregate stability

In this study, three different methods, i.e., pipette method, wet sieving, and rainfall simulation were used to assess aggregate stability. At each method, for quantitatively calculating the soil interparticle forces, we directly used the NaCl with a concentration of 10^{-4}, 10^{-3}, 10^{-2}, 10^{-1}, and 1 mol L^{-1} as wetting medium, and the wide concentration range was in order to involve the all possible interparticle forces in the field soils.

Aggregate stability tested by pipette method was following the study of Xu et al. (2015). In brief, 20 g Na^+ saturated 1–5 mm macroaggregates were immersed in a 500 mL cylinder containing NaCl solution, next turned the cylinder to uniformly distribute the soil particles and then left to settle. According to the Stokes law, after a corresponding time, fine particles of diameters <20, <10, and <5 μm were sucked, and the suspensions were oven-dried and weighed. Finally, the mass percentage of the released fragments with diameters of >20, >10 and >5 μm, defined as aggregate stability index (ASI), was determined through the following equation (Xu et al., 2015; Yu et al., 2020b). Three replicates were prepared for each run.

$$W(>d)\% = 1 - \frac{(m - V \times c_0 \times M_W) \times \frac{0.5}{V} \times 2}{20} \times 100\% \quad (1)$$

where W (>d) (%) is the mass percent of the released fragments with diameters higher than d ($d = 5$, 10, and 20 μm) relative to the total mass of aggregates; m (g) is the total mass of NaCl and released fragments in the extracted suspension; c_0 (mol L^{-1}) is the molar concentration of NaCl; M_w (g mol^{-1}) is the molecular weight of NaCl, and V (L) is the

Table 1
Basic physical and chemical properties of soil samples used in present study.

Soil type	CEC cmol kg^{-1}	SSA m^2 g^{-1}	SOM g kg^{-1}	pH	Sand (2–0.02 mm) %	Silt (0.02–0.002 mm) %	Clay (<0.002 mm) %
Loessal soil	7.2	23.0	4.6	8.6	76.7	15.3	8.0
Lou soil	23.2	41.5	14.5	8.0	34.0	40.6	25.4
Cinnamon soil	19.6	42.3	24.1	7.9	28.0	44.8	27.2
Heilu soil	18.3	49.5	25.1	8.0	43.9	36.6	19.5

CEC: cation exchange capacity; SSA: specific surface area; SOM: soil organic matter.

volume of the extracted suspension. 0.5 (L) is the volume of the whole suspension. The constant 2 was incorporated because, in the process of sedimentation, almost half of the target particles (in diameter of $< d$) remained in the extracted suspension while the other half had moved below the sampled portion by sedimentation.

Aggregate stability tested by wet sieving was referred to the fast treatment as described by Le Bissonnais (1996). 5 g Na^+ saturated macroaggregates (1–5 mm) were first immersed in 50 mL NaCl electrolyte solution for 10 min, then removing the electrolyte solution and sieving (1, 0.5, 0.25, 0.15, and 0.053 mm) in ethanol. Finally, sieve retained aggregates were oven dried and weighed to calculate the mean weighted diameter (MWD) following Eq. (2). Three replicates of each soil were conducted.

$$MWD = \sum_{i}^{n+1} \frac{r_{i+1} + r_i}{2} \times m_i \tag{2}$$

where r_i is the diameter of the ith sieve (mm), $r_0 = r_1$, $r_n = r_{n+1}$, and m_i is the retained mass percentage in the ith sieve.

Aggregate stability was also measured by rainfall simulation. The device and experimental procedures for this method were set as described by the study of Hu et al. (2018b). The mean raindrop size was 2.5 mm and the rainfall intensity was 60 mm h^{-1}. Prior to rainfall, uniform loading of Na^+-saturated macroaggregates (1–5 mm) onto the circular sieve was performed. As the rainfall started, fragments of splashed aggregate were gathered at intervals of 30 s. When the soil surface was covered by the water film, the experiment was stopped. Thereafter, splashed soil particles were oven-dried and weighed. Each soil type was conducted in three replications.

2.4. Quantitative calculation of soil interparticle forces

Net pressure (P_{net}) denotes the sum of electrostatic repulsive pressure (P_e), hydration repulsive pressure (P_h), and van der Waals forces (P_{vdw}), which can be calculated using the following equations (Li et al., 2013; Hu et al., 2015):

$$P_{net} = P_{vdw} + P_h + Pe \tag{3}$$

$$P_{vdw} = -\frac{A}{6\pi d^3} \times 10^{22} \tag{4}$$

$$P_h = 3.3 \times 10^4 e^{-5.76d} \tag{5}$$

$$P_e = \frac{2}{101} RTc_0 \left\{ cosh\left[\frac{ZF\phi(d/2)}{RT}\right] - 1 \right\} \tag{6}$$

where d (nm) is the adjacent particles spacing; A (J) is effective Hamaker constant in aqueous solution; R (J mol^{-1} K^{-1}) is gas constant; T (K) is absolute temperature; F (C mol^{-1}) is Faraday constant; Z is cation valence; c_0 (mol L^{-1}) is the equilibrium concentration of the cation in the bulk solution; φ (d/2) (V) is the potential at the middle of the overlapping position of the electric double layers of two adjacent particles, which can be calculated using the following equation (Yu et al., 2017; Ding et al., 2019)

$$\frac{\pi}{2}\left[1 + \left(\frac{1}{2}\right)^2 e^{\frac{2ZF\phi(d/2)}{RT}} + \left(\frac{3}{8}\right)^2 e^{\frac{4ZF\phi(d/2)}{RT}}\right] - arcsine^{\frac{ZF\phi_0 - ZF\phi(d/2)}{2RT}} = \frac{1}{4} d\kappa e^{\frac{-ZF\phi(d/2)}{2RT}} \tag{7}$$

where

$$\kappa = \left(10^{-15} \times 8\pi F^2 c_0/\varepsilon RT\right)^{1/2} \tag{8}$$

κ (1/nm) is the Debye-Hückel parameter, κ^{-1} (nm) represents the electric double layer thickness.

3. Results

3.1. Soil interparticle forces

The net pressure of the soil interparticle forces is shown in Fig. 1. The positive and negative values represent the net attractive and repulsive pressure, respectively. When the particle spacing is within 1 nm, at any NaCl concentration, the net pressure of the four soils is always repulsive and more than 100 atm. For example, when the particle spacing is 0.6 nm, the net repulsive force is about 1000 atm. In this study, the net attractive pressure for Heilu soil, Cinnamon soil, Lou soil, and Loessal soil was only found with 1 mol L^{-1} NaCl concentration and particles spacing was higher than 1.5, 1.6, 1.7 and 1.9 nm, respectively. These results indicate that the soil particles were easier to agglomerate for Heilu soil than the other three soils. Additionally, at the same particle spacing, the net pressure increased with decreasing concentration of NaCl solution. Specifically, as the NaCl concentration was $\leq 10^{-2}$ mol L^{-1}, overlapping of net pressure curves occurred, indicating that it was a critical concentration of the net pressure.

To further investigate the impact of the NaCl concentration on soil interparticle net pressure, the net pressure at the particle spacing of 1.5 nm and under various NaCl concentrations was directly plotted (Fig. 2). As shown in Fig. 2, for the four soils, the net repulsive pressure displayed rapid growth at first and then remained nearly no change with decreasing NaCl concentration, it can be clearly seen that the 10^{-2} mol L^{-1} was the critical concentration for the net repulsive pressure in four soils. With 1 mol L^{-1} NaCl concentration, the net repulsive pressure for Heilu soil, Cinnamon soil, Lou soil, and Loessal soil was 0, 2.17, 4.93, and 8.34 atm, respectively. With the decline in concentration up till 10^{-2} mol L^{-1}, the net repulsive pressure for these four soils was 24.40, 28.79, 32.06, and 32.52 atm, and the increment was 24.40, 26.14, 26.65 and 24.70 atm, respectively. However, when NaCl concentration decreased from 10^{-2} to 10^{-4} mol L^{-1}, only 0.48 atm increment occurred in net repulsive pressure. Moreover, Fig. 2 exhibits that the decreasing order of net repulsive pressure of the four soils was Loessal soil > Lou soil > Cinnamon soil > Heilu soil.

3.2. Soil aggregate stability determination using different methods

Aggregate stability measured by the pipette method was characterized by the aggregate stability index (ASI), which was defined as the mass content of fragments with diameters higher than 5, 10, or 20 μm released from Na^+ saturated aggregate. The higher the ASI, the bigger the stability of aggregates. Fig. 3 shows the relationship between the ASI

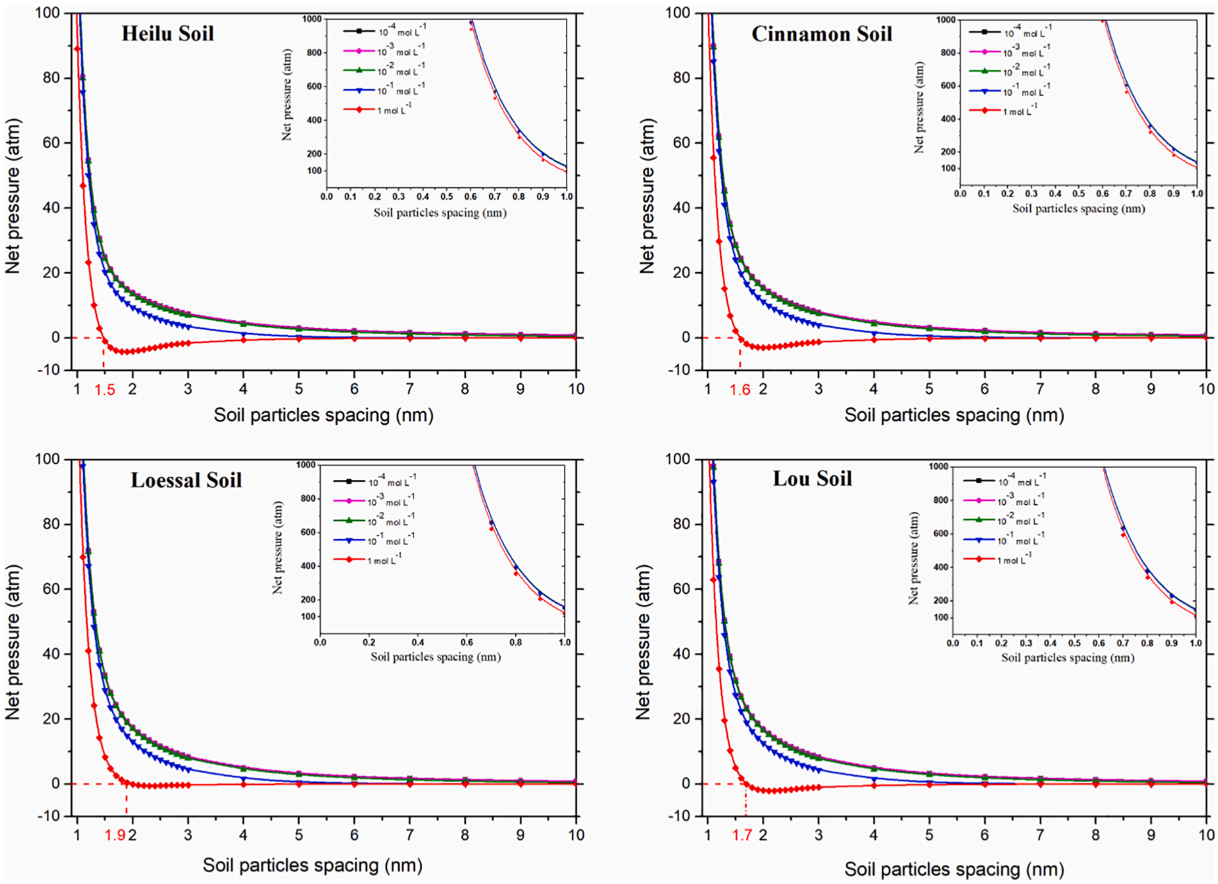

Fig. 1. Distribution of net interparticle forces between two adjacent particles under various concentrations of NaCl solution.

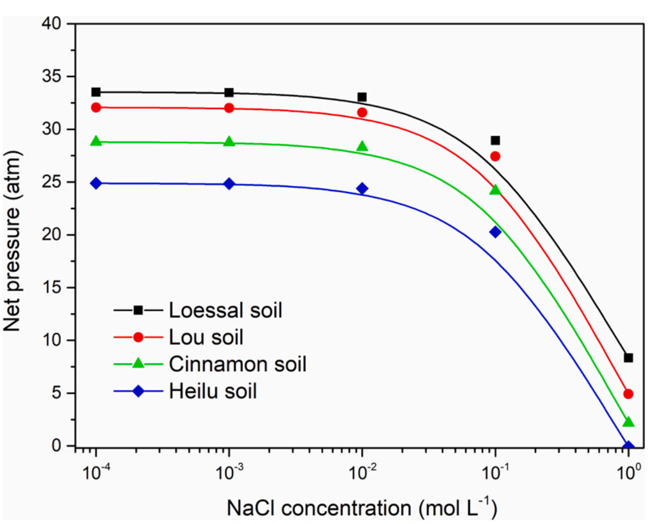

Fig. 2. Net forces at the particle spacing of 1.5 nm under various NaCl concentrations.

and the NaCl solution concentration. The results show that for all size fractions (>5, 10 or > 20 μm), the mass content of released fragments was nearly unchanged at first and then increased remarkably with NaCl concentration increased, and the concentration at the intersection point was 10^{-2} mol L^{-1} considering as a crucial concentration for aggregate stability.

According to the ASI, the difference in four soils' aggregate stability was different in various concentrations. When the NaCl concentration was < 10^{-2} mol L^{-1}, the mass content of released fragments (>5, 10, or > 20 μm) was higher in Loessal soil than in Lou soil and Heilu soil, and the smallest content was found in Cinnamon soil. This implies that the aggregate stability decreased in the order Loessal soil > Heilu soil, Lou soil > Cinnamon soil, under these concentrations. With 10^{-1} mol L^{-1} NaCl solution, for all size fractions, the difference in aggregate stability between Heilu soil, Lou soil, and Cinnamon soil was small, and the stability of these three soil aggregates were all lower than that of Loessal soil aggregates. While the concentration of NaCl solution was 1 mol L^{-1}, fragments released from four soils were all higher than 5 μm, and the difference of aggregate stability between Loessal soil and the other three soils was close to zero.

Soil aggregate stability evaluated by the wet sieving method was expressed in terms of MWD. The higher value of MWD represents the higher stability of soil aggregate. Fig. 4 shows the relationship between MWD and NaCl concentration. It can be seen that the change in the value of MWD was much greater for the concentration above 10^{-2} mol L^{-1} than that of below 10^{-2} mol L^{-1}. There was a critical concentration of 10^{-2} mol L^{-1} for the four soils aggregate stability. When NaCl concentration was between 10^{-2} and 1 mol L^{-1}, aggregate stability increased at a high rate with increasing NaCl concentration. The increments in MWD for Heilu, Lou, Loessal, and Cinnamon soil was 0.13, 0.13, 0.15, and 0.11 mm, respectively. However, when the NaCl concentration was between 10^{-4} and 10^{-2} mol L^{-1}, a very small difference was observed in MWD values at various concentrations. The decrement in MWD from NaCl of 10^{-2} to 10^{-4} mol L^{-1} concentration was only 0.01, 0.02, 0.02, and 0 mm for Heilu, Lou, Loessal, and Cinnamon soils, respectively. Based on MWD values, the order of aggregate stability for the four soils was as follows: Heilu soil > Lou soil > Loessal soil > Cinnamon soil.

Soil aggregate stability tested by the rainfall simulation method was expressed by the splash erosion mass (SE). Soil aggregate stability decreased with increasing SE. Fig. 5 shows the changing curve of SE with

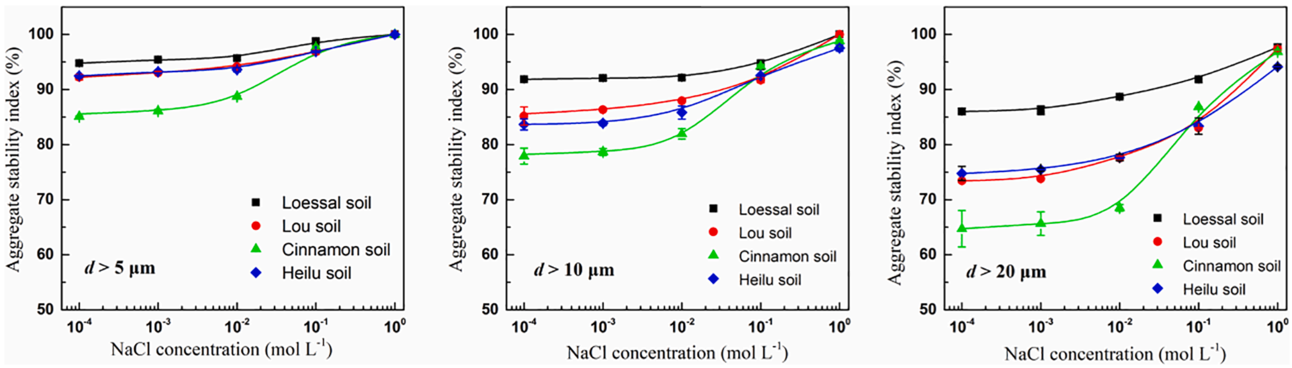

Fig. 3. Soil aggregate stability index (ASI) at different NaCl concentrations as measured by using the pipette method.

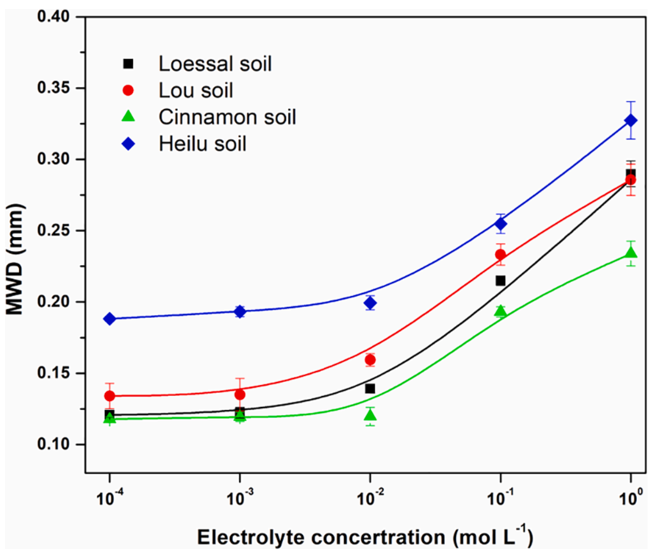

Fig. 4. Mean weight diameter (MWD) at different NaCl concentrations as measured by using the wet sieving method.

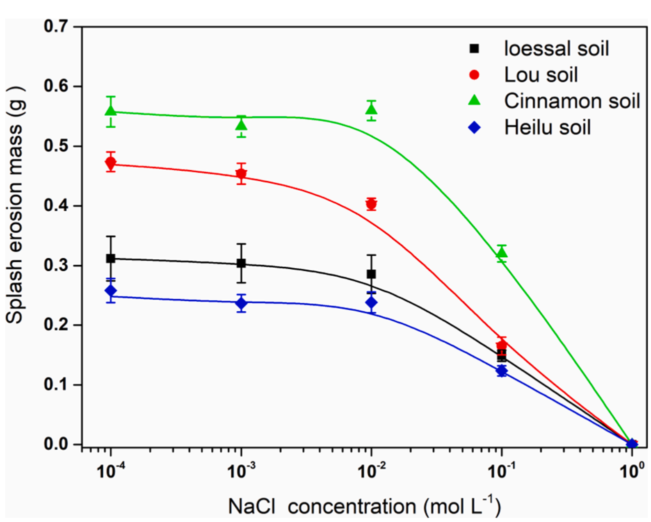

Fig. 5. Splash erosion mass (SE) at different NaCl concentrations as measured by using the rainfall simulation method.

NaCl concentration of the four soils. In the presence of 1 mol L^{-1} NaCl solution, no splashed out of any soil particle occurred, which means that the aggregates were rather stable at this electrolyte concentration. With a decrease in NaCl concentration from 1 to 10^{-2} mol L^{-1}, SE of Cinnamon, Lou, Loessal, and Heilu soil rapidly increased from 0 to 0.56, 0.40, 0.29, and 0.24 g, respectively. However, when NaCl concentration was further decreased till 10^{-4} mol L^{-1}, the very small increment of SE in four soils was occurred, with values less than 0.05 g. This changing trend reveals that the NaCl concentration with 10^{-2} mol L^{-1} is the turning point for the stability of aggregate in four soils. Furthermore, according to SE values of the four soils, the order of aggregate stability at any NaCl concentration was as follows: Heilu soil > Loessal soil > Lou soil > Cinnamon soil.

3.3. Correlation between soil aggregate stability indicators obtained from different methods

Table 2 displays the correlation between soil aggregate stability indicators obtained from different methods. Here, for the pipette method, the mass percentage of aggregate fragments with a diameter higher than 20 μm were used for correlation analysis. As shown in Table 2, the correlations between the indicators of soil aggregate stability were extremely remarkable for the four soils ($P < 0.01$). MWD tested by wet sieving and ASI tested by pipette method exhibited a significant positive correlation, while the correlation is significantly negative between SE tested by rainfall simulation and ASI tested by pipette method, and MWD and SE. The correlation coefficients in all four soils were lower than these in a single soil. The strongest correlation was observed between SE and ASI in the Lou soil (r = –0.98).

4. Discussion

4.1. Effects of soil interparticle forces on aggregate stability

In the present research, the impact of soil interparticle froces in aggregate stability was evaluated by wet sieving, rainfall simulation and pipette method. The changing law of soil aggregate stability with NaCl concentration measured by the three methods was identical, that is, soil aggregate stability decreased at a high rate with decreasing NaCl concentration from 1 to 10^{-2} mol L^{-1}, and then basically remained unchanged with further decrease till 10^{-4} mol L^{-1}, indicating critical

Table 2
Pearson correlation between aggregate stability indicators obtained from different methods.

Pearson coefficient	Loessalsoil	Lou soil	Cinnamon soil	Heilu soil	All soils
ASI *vs* MWD	0.97**	0.96**	0.95**	0.96**	0.69**
ASI *vs* SE	–0.92**	–0.98**	–0.91**	–0.92**	–0.84**
MWD *vs* SE	–0.96**	–0.98**	–0.95**	–0.94**	–0.88**

ASI: aggregate stability index, MWD: mean weight diameter, SE: splash erosion mass;**P < 0.01.

electrolyte concentration of 10^{-2} mol L^{-1} for aggregate stability. These results are in keeping with past findings (Xu et al., 2015; Yu et al., 2017; Hu et al., 2018a, 2018b). In addition, the experimental results of aggregate stability measured through these methods completely coincided with the theoretical calculation of soil net interparticle pressure. In the presence of the concentration lesser than the critical point, the net repulsive pressure revealed a little change which is also corresponding to the minor change in aggregate stability. While with a higher concentration than the critical point, the net repulsive pressure considerably increased, thereby, the aggregate stability rapidly decreased. This indicates that the soil interparticle forces exhibited imperative impact on aggregate stability. In the field, when aggregate is dry, the electrolyte concentration in soil bulk solution is very high. Under this case, the thickness of the electric double layer, i.e., Debye length is small, resulting in a weak repulsive force between particles, thus the aggregate is very stable. When the rainfall or irrigation water enters the soil, the increasing water content within the aggregate can lead to a decreasing electrolyte concentration. Under those circumstances, the electric double layer thickness increased due to the weak ability of lower concentration electrolytes to screen the electric field, meaning that the repulsive force between particles is strengthened, and hence the aggregates break down. Therefore, the disintegration of natural aggregate by water may be due to the increased interparticle repulsive pressure within the aggregate.

In general, raindrop impact forces, slaking effects, clay swelling effects, and physico-chemical dispersion influence aggregate breakdown during the wetting process (Le Bissonnais, 1996). Raindrop impact force and slaking effect have long been considered as the main force inducing aggregate breakdown (Ramos et al., 2003; Jimba and Lowery, 2010; Fernández-Raga et al., 2018). However, according to our results (Figs. 3 and 4), soil aggregates could break apart when there was no raindrop impact force, indicating that raindrop impact force is not necessary for soil aggregate breaking. In addition, past studies reported that raindrop impact force was just 1 to 3 atm, and during the process of wetting the air pressure within the aggregates was less than 1 atm (Nearing et al., 1987; Zaher et al., 2005). In contrast, the attractive force among soil particles can usually be 100–1000 atm (Li et al., 2013; Hu et al., 2015). Therefore, the disparity in the intensity of the forces implies that raindrop impact force and slaking effect are impossible to directly break apart soil aggregates. The work of Le Bissonnais (1996) found that the destructive effect of raindrop impact on aggregate was dominant only in wet soils. When the soil was wetted, physico-chemical dispersion has been worked due to the change of soil solution chemical properties such as electrolyte concentration. Physico-chemical dispersion mainly comes from the interaction forces between soil particles (Le Bissonnais, 1996; Yu et al., 2017). Many studies have reported that surface hydration and electrostatic repulsive forces were capable to reach up to hundreds of thousands of atmospheres, indicating that soil internal force is strong enough to breakdown soil aggregates (Li et al., 2013; Xu et al., 2015; Yu et al., 2017). Similarly, our results showed that the net repulsive force was approximately 1000 atm when the soil particle spacing was 0.6 nm, which was much stronger than the raindrop impact force and slaking effect. Yu et al. (2020a) also reported that in every soil type, the soil internal forces are responsible to control its aggregate stability (i.e., permanently and variably charged soils). Overall, it was the soil interparticle forces that initiated aggregate breakdown.

4.2. Methods for evaluating soil aggregate stability

In this study, we found that all three methods can be effectively utilized to assess the impacts of soil interparticle forces on aggregate stability. Significant relationships existed between the indicators tested by the methods ($P < 0.01$), and their r values were all > 0.89 for each soil type (Table 2). A similar result was observed by Nouwakpo et al. (2018), who also mentioned that aggregate stability tested via wet sieving was a good predictor of soil loss obtained from rainfall simulation experiments. In addition, high correlations between the indicators tested by the methods used in the present study infer that soil aggregates experienced the same breakdown mechanisms in these three methods.

Pipette method is regarded as a classical method to study the effects of physical-chemistry on aggregate stability (Le Bissonnais, 1996; Ding et al., 2019). In this study, stability of aggregate tested by the pipette method is represented by the ASI, which refers to the mass percent of released fragments with diameters of > 5, > 10 and > 20 μm from soil macroaggregates (Xu et al., 2015; Yu et al., 2020b). The higher value of ASI meant the less fine particles be released, indicating that the aggregate was more stable. The results of the ASI show that as the NaCl concentration was smaller than 10^{-2} mol L^{-1}, the stability of four soil aggregates decreased in the order: Loessal soil > Heilu soil, Lou soil > Cinnamon soil (Fig. 3). While the NaCl concentration was bigger than 10^{-2} mol L^{-1}, the difference in aggregate stability between Loessal soil and the other three soils decreased to zero with increasing NaCl concentration. These results might be explained by the difference in interparticle forces and particle size distribution between soils. When the concentration of NaCl was lower than 10^{-2} mol L^{-1}, the net repulsive pressure was strong, and the highest net repulsive pressure occurred in Loessal soil (Figs. 2 and 3). According to the study of Le Bissonnais. (1996), the fragments resulting from the strong repulsive forces were mainly elementary particles. In this method, the maximum particle size measured was 20 μm, which was exactly the lower limit of the sand. Thus, the value of ASI was very sensitive to the sand content under these circumstances. For instance, the sand content in Loessal soil was 2.82 times higher than that in Cinnamon soil (Table 1), which may result in the aggregate stability index in Loessal soil higher than in Cinnamon soil (Fig. 3). Thus, Cinnamon soil seems to be the least stable soil, whereas Loessal soil seems to be the most stable soil. With the higher concentration of NaCl than 10^{-2} mol L^{-1}, the soil net repulsive force decreased due to the increasing concentration lead to the increased size of fragments released from the saturated aggregate, thus reducing the difference in the value of ASI between Loessal soil and the other three soils. Based on the above discussion, pipette method, as a classical method, was the most accurate method for evaluating the impact of strong repulsive forces on the stability of aggregate, but it was not appropriate for comparing the difference in aggregate stability between soils.

Wet sieving method was a simple and time-saving method to determine aggregate stability. This method characterizes aggregate stability with MWD, which is a comprehensive indicator of aggregates of all sizes (Amézketa, 1999; An et al., 2013; Zeng et al., 2018). A higher value of MWD represents the higher stability of the aggregate. The descending order of soil aggregate stability determined through MWD was Heilu soil > Lou soil > Loessal soil > Cinnamon soil, which differed from the order determined by pipette method. This may be due to the fact that the value of MWD largely depends on the fragments with bigger size. The weak relationship between the wet sieving and pipette methods ($R^2 = 0.4773$, Fig. 6), determined by regression analysis, also revealed that the fine particles had less impact on MWD. Therefore, a small content of bigger fragments could considerably increase MWD.

Organic matter, composed of microbial decomposition products, extracellular polymers, root exudates, etc., as the key binding agent has a positive impact on the formation and stability of soil aggregate (Zeng et al., 2018; Liu et al., 2020). Huang (2004) reported that organic matter improves aggregate stability by increasing the van der Waals forces between particles. Similar outcomes were also reported by Yu et al. (2017), who found that the addition of organic materials to soil decreased electric repulsive force and increased van der Waals force. Hence, organic matter inputs could reduce net repulsive pressure between soil particles, thereby decreasing the degree of aggregate breakdown and producing the bigger fragments. This may be the reason that the aggregate of Heilu soil with the high organic matter content (25.1 g kg^{-1}) detected by wet sieving was the most stable. In addition, considering that fragments caused by strong repulsive force were generally the

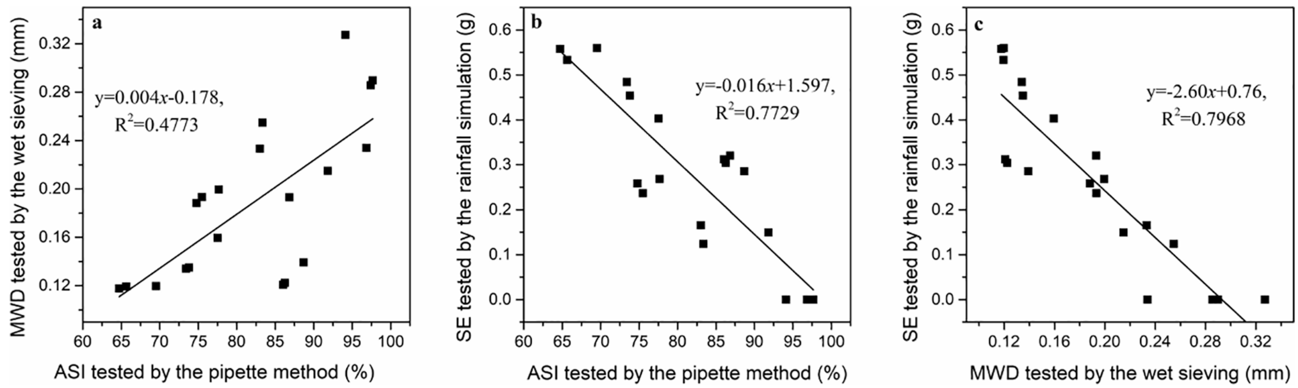

Fig. 6. Regression analysis between soil aggregate stability indicators obtained from different methods. ASI: aggregate stability index; MWD: mean weight diameter; SE: splash erosion mass.

primary particles, as such, soil particle composition was another important factor affecting the stability of aggregates subjected to soil internal forces. This study revealed that the stability of Loessal soil with the lowest organic matter content (4.97 g kg^{-1}) seemed higher than that of Cinnamon soil with high organic matter content (24.11 g kg^{-1}). This may be because the highest content of sand particles occurred in Loessal soil, which was 2.87 times higher than that in Cinnamon soil (Table 1). Therefore, when using the wet sieving method to compare the differences in aggregate stability between soils, the sand content may be an interference factor for the value of MWD.

Rainfall Simulation method determined the order of soil aggregate stability as follows: Heilu soil > Loessal soil > Lou soil > Cinnamon soil. The rainfall Simulation method characterizes aggregate stability using SE, which is the mass of soil particles moved by raindrop impact. In our past study, we found that soil interparticle forces initiate aggregate breaking and thus provide fine particles to splash by the raindrop (Hu et al., 2018a, 2018b). Therefore, except soil interparticle forces, the raindrop impact as a driving force for soil particle movement also had an imperative influence on splash erosion mass (Le Bissonnais and Singer, 1993; Legout et al., 2005; Hu et al., 2018a). The value of SE is significantly influenced by raindrop size and shape, kinetic energy, and intensity (Wei et al., 2007; Fu et al., 2016; Xiao et al., 2018; Fernández-Raga et al., 2018). However, in the present study, raindrop properties were similar, and SE was mainly determined by the number of fine soil fragments. Therefore, like the result of wet sieving method, the aggregate stability of Heilu soil was the highest. This was because Heilu soil had the lowest net repulsive pressure among the four soils (Figs. 1 and 2).

According to the above discussion, although the disintegration of four soil aggregates were all resulting from the interparticle forces, the order of aggregate stability showed differences among the four soils using different methods. Similarly, Amézketa (1999) presented that the ranking of soil aggregates stability based on the parameters obtained with the unified method proposed by Le Bissonnais (1996) was not the ranking obtained by wet sieving. Saygin et al. (2015) and Almajmaie et al. (2017) further revealed that there was no single method of testing aggregate stability can be suitable to all soil types and circumstances. This result was confirmed by our study, which reveals that it was still challenging to select an appropriate method to compare the differences in the aggregate stability of all soil types. Even though the breakdown mechanisms are the same, differences in aggregate stability between methods can still cause by the expression of stability data obtained from the methods, and the intrinsic features of studied soils, such as soil organic content and particle size distribution (Rohoskova, 2004; Pulido Moncada et al., 2015; Saygin et al., 2015; Almajmaie et al., 2017). Therefore, for the comparison purpose, multiple methods should be considered to evaluate the impact of soil interparticle forces on stability of different soils. If a single method was to be chosen, the method of wet sieving may be a good choice due to the time savings, simple procedure, and comprehensive information about released fragments sizes and amount.

5. Conclusions

In this study, wet sieving, rainfall simulation and pipette method were utilized to measure the impacts of soil interparticle forces on stability of aggregate. All three methods could be used to assess the impact of soil interparticle forces on stability of aggregate. However, there is no single method that can be valid for a wide range of soil types. Among the three methods, pipette method is the classical and accurate method to study the influence of soil interparticle forces on aggregate stability, but it is not appropriate to compare the aggregate stability of different soil types. For the comparison purpose, multiple methods should be considered. If a single method was to be selected to evaluate the impact of soil interparticle forces in stability of different soil aggregates, the wet sieving method may be a good choice because it was not only relatively time-saving and simple, but also reflected more comprehensive information about sizes and amount of fragments released from soil aggregates. In addition, rainfall simulation method which linked the aggregate stability with soil erosion was recommended to study the relationship between them.

Declaration of Competing Interest

The authors declare that they have no known competing financial interests or personal relationships that could have appeared to influence the work reported in this paper.

Acknowledgements

This work was supported by the National Key R&D Program of China (2016YFE0202900), and the National Natural Science Foundation of China (41977024, 41601236 and 41701261).

Appendix A. Supplementary data

Supplementary data to this article can be found online at https://doi.org/10.1016/j.geoderma.2020.114834.

References

Almajmaie, A., Hardie, M., Acuna, T., Birch, C., 2017. Evaluation of methods for determining soil aggregate stability. Soil Tillage Res. 167, 39–45.
Amézketa, 1999. Soil Aggregate Stability, A Review. Journal of Sustainable Agriculture. 14 (2–3), 83–151.
An, S.S., Darboux, F., Cheng, M., 2013. Revegetation as an efficient means of increasing soil aggregate stability on the Loess Plateau (China). Geoderma 209, 75–85.

Barthès, B., Roose, E., 2002. Aggregate stability as an indicator of soil susceptibility to runoff and erosion; validation at several levels. Catena 47 (2), 133–149.

Bruce-Okine, E., Lal, R., 1975. Soil erodibility as determined by the raindrop technique. Soil Sci. 119, 149–157.

Cantón, Y., Solé-Benet, A., Asensio, C., Chamizo, S., Puigdefábregasb, J., 2009. Aggregate stability in range sandy loam soils Relationships with runoff and erosion. Catena 77 (3), 192–199.

Ding, W.Q., Liu, X.M., Hu, F.N., Zhu, H.L., Luo, Y.X., Li, S., 2019. How the particle interaction forces determine soil water infiltration: specific ion effects. J. Hydrol. 568, 492–500.

Falsone, G., Bonifacio, E., Zanini, E., 2012. Structure development in aggregates of poorly developed soils through the analysis of the pore system. Catena 95 (1), 169–176.

Fernández-Raga, M., Palencia, C., Keesstra, S. Antonio, Jordán., Artemi, Cerdà., 2018. Splash erosion, A review with unanswered questions. Earth-Science Reviews. 171, 463–477.

Fu, Y., Li, G., Zheng, T., Li, B., Zhang, T., 2016. Impact of raindrop characteristics on the selective detachment and transport of aggregate fragments in the Loess Plateau of China. Soil Sci. Soc. Am. J. 80 (4), 1071–1077.

Herrick, J.E., Whitford, W.G., Soyza, A.G., Van Zee, J.W., Havstad, K.M., Seybold, C.A., Walton, M., 2001. Field soil aggregate stability kit for soil quality and rangeland health evaluations. Catena 44, 27–35.

Horn, R., Smucker, A., 2005. Structure formation and its consequences for gas and water transport in unsaturated arable and forest soils. Soil Tillage Res. 82 (1), 5–14.

Huang, P.M., 2004. Soil mineral-organic matter-microorganism interactions: fundamentals and impacts. Adv. Agron. 82, 391–472.

Huang, X.R., Li, H., Li, S., Jiang, X.J., 2016. Role of cationic polarization in humus-increased soil aggregate stability. Eur. J. Soil Sci. 67 (3), 341–350.

Hu, F.N., Xu, C.Y., Li, H., Li, S., Yu, Z.H., Li, Y., He, X.H., 2015. Particles interaction forces and their effects on soil aggregates breakdown. Soil Tillage Res. 147, 1–9.

Hu, F.N., Liu, J.F., Xu, C.Y., Wang, Z.L., Liu, G., Li, H., Zhao, S.W., 2018a. soil internal forces initiate aggregate breakdown and splash erosion. Geoderma 320, 43–51.

Hu, F.N., Liu, J.F., Xu, C.Y., Du, W., Yang, Z.H., Liu, X.M., Liu, G., Zhao, S.W., 2018b. soil internal forces contribute more than raindrop impact force to rainfall splash erosion. Geoderma 330, 91–98.

Jimba, S.C., Lowery, B., 2010. Automation of the water-drop method for soil aggregate stability analysis. Soil Sci. Soc. Am. J. 74 (1), 38–41.

Kemper,W., Rosenau, R., 1986. Aggregate stability and size distribution, In: Klute, A. (Ed.), Methods of Soil Analysis. 2nd ed. ASA, Madison, WI, pp. 425–442 (Agronomy Monograph 9).

Le Bissonnais, Y., Singer, M.J., 1993. Seal formation, runoff, and interrill erosion from seventeen California soils. Soil Sci. Soc. Am. J. 57 (1), 224–229.

Le Bissonnais, Y., 1996. Aggregate stability and assessment of soil crustability and erodibility, I. Theory and methodology. Eur. J. Soil Sci. 47 (4), 425–437.

Legout, C., Leguedois, S., Le B, Y., 2005. Aggregate breakdown dynamics under rainfall compared with aggregate stability measurements. European Journal of Soil Science. 56 (2), 225–238.

Leng, Y., 2012. Hydration force between mica surfaces in aqueous KCl electrolyte solution. Langmuir 28 (12), 5339–5349.

Levy, G.J., Mamedov, A.I., Goldstein, D., 2003. Sodicity and water quality effects on slaking of aggregates from semi-arid soils 1. Soil Sci. 168 (8), 552–562.

Li, H., Hou, J., Liu, X.M., Li, R., Zhu, H., Wu, L.S., 2011. Combined determination of specific surface area and surface charge properties of charged particles from a single experiment. Soil Sci. Soc. Am. J. 75 (6), 2128–2135.

Li, S., Li, H., Xu, C.Y., Huang, X.R., Xie, D.T., Ni, J.P., 2013. Particle interaction forces induce soil particle transport during rainfall. Soil Sci. Soc. Am. J. 77 (5), 1563.

Liang, Y., Hilal, N., Langston, P., Starov, V., 2007. Interaction forces between colloidal particles in liquid, Theory and experiment. Adv. Colloid Interface Sci. 134 (21), 151–166.

Liu, J.F., Wang, Z.L., Hu, F.N., Xu, C.Y., Ma, R.T., Zhao, S.W., 2020. Soil organic matter and silt contents determine soil particle surface electrochemical properties across a long-term natural restoration grassland. Catena 190.

McBride, M.B., Baveye, P., 2002. Diffuse double-layer models, long-range forces, and ordering in clay colloids. Soil Sci. Soc. Am. J. 66, 1207–1217.

Nearing, M.A., Bradford. J.M., Holtz, R.D., 1987. Measurement of Waterdrop Impact Pressures on Soil Surfaces. 51(5), 1302–1306.

Nouwakpo, S.K., Song, J., Gonzalez, J.M., 2018. Soil structural stability assessment with the fluidized bed, aggregate stability, and rainfall simulation on long-term tillage and crop rotation systems. Soil Tillage Res. 2018 (178), 65–71.

Pulido Moncada, M., Gabriels, D., Cornelis, W., Lobo, D., 2015. Comparing aggregate stability tests for soil physical quality indicators. Land Degrad. Dev. 26 (8), 843–852.

Quirk, J.P., 1950. The measurement of stability of soil micro-aggregatesin water. Aust. J. Agric. Res. 1, 276–284.

Ramos, M.C., Nacci, S., Pla, I., 2003. Effect of raindrop impact and its relationship with aggregate stability to different disaggregation forces. Catena 53 (4), 365–376.

Rohoskova, M., 2004. Comparison of two methods for aggregate stability measurement: a review. Plant Soil Environ. 50 (8), 379–382.

Saygin, S.D., Erpul, G., Basaran, M., 2015. Comparison of aggregate stability measurement methods for clay-rich soils in a sartepe catchment of turkey. Land Degrad. Dev. 28, 199–206.

Vaezi, A.R., Ahmadi, M., Cerdà, A., 2017. Contribution of raindrop impact to the change of soil physical properties and water erosion under semi-arid rainfalls. Sci. Total Environ. 583, 382–392.

Wei, W., Chen, L.D., Fu, B.J., Huang, Z.L., Wu, D.P., Gui, L.D., 2007. The effect of land uses and rainfall regimes on runoff and soil erosion in the semi-arid loess hilly area, China. J. Hydrol. 335 (3), 247–258.

Xiao, H., Liu, G., Zhang, Q., Zheng, F.L., Zhang, X.C., Liu, P.L., 2018. Quantifying contributions of slaking and mechanical breakdown of soil aggregates to splash erosion for different soils from the Loess plateau of China. Soil Tillage Res. 178.

Xu, C.Y., Yu, Z.H., Li, H., 2015. The coupling effects of electric field and clay mineralogy on clay aggregate stability. J. Soils Sediments 15 (5), 1159–1168.

Yang, X., Zhang, Q., Li, X., Jia, X., Wei, X., Shao, M.A., 2015. Determination of soil texture by laser diffraction method. Soil Sci. Soc. Am. J. 79 (6), 1556–1566.

Yoder, R.E., 1936. A direct method of aggregate analysis of soil and a study of nature of erosion losses. J. Am. Soc. Agron. 28 (5), 337–351.

Yu, Z.H., Zhang, J., Zhang, C., Xin, X., Li, H., 2017. The coupling effects of soil organic matter and particle interaction forces on soil aggregate stability. Soil Tillage Res. 174, 251–260.

Yu, Z.H., Zheng, Y.Y., Zhang, J.B., Zhang, C.Z., Ma, D.H., Chen, L., Cai, T.Y., 2020a. Importance of soil interparticle forces and organic matter for aggregate stability in a temperate soil and a subtropical soil. Geoderma 362, 114088.

Yu, L.Q., Tian, R., Zhang, R.H., Liu, X.M., Li, R., Li, H., 2020b. Coupling effects of humus and 2:1 type electrolyte on soil water movement. Geoderma 375, 114482.

Zaher, H., Caron, J., Ouaki, B., 2005. Modeling aggregate internal pressure evolution following immersion to quantify mechanisms of structural stability. Soil Sci. Soc. Am. J. 69 (1), 1–12.

Zeng, Q.C., Darboux, Frederic, Man, C., Zhu, Z.L., An, S.S., 2018. Soil aggregate stability under different rain conditions for three vegetation types on the Loessal Plateau (China). Catena 167, 276–283.

Zhu, Z,L., Minasny, B.B., Field, D.J., 2009. Measurement of aggregate bond energy using ultrasonic dispersion. European Journal of Soil Science. 60 (4), 695–705.